Available online at www.sciencedirect.com
ScienceDirect
Bioorganic & Medicinal Chemistry Letters 16 (2006) 5809–5813
Bioorganic & Medicinal Chemistry Letters

p38 MAP kinase inhibitors. Part 6: 2-Arylpyridazin-3-ones as templates for inhibitor design

Swaminathan R. Natarajan,[a,*] Stephen T. Heller,[a] Kiyean Nam,[a] Suresh B. Singh,[a] Giovanna Scapin,[a] Sangita Patel,[a] James E. Thompson,[b] Catherine E. Fitzgerald[b] and Stephen J. O'Keefe[b]

[a]*Department of Medicinal Chemistry, Merck Research Laboratories, PO Box 2000, Rahway, NJ 07065, USA*
[b]*Department of Inflammation Research, Merck Research Laboratories, PO Box 2000, Rahway, NJ 07065, USA*

Received 15 July 2006; revised 15 August 2006; accepted 15 August 2006
Available online 30 August 2006

Abstract—p38 inhibitors based on 3,4-dihydropyrido[4,3-*d*]pyrimidazin-2-one template were synthesized and their SAR explored. Benchmark compounds **30**, **35**, and **36** were found to be potent against the enzyme. Crystal structure of p38 in complex with **30** indicated a key π-stacking interaction with the pendant tyrosine residue-35 in the glycine-rich loop.

It has been shown that inhibition of p38 MAP kinase is key to blocking the pro-inflammatory signal transduction cascade initiated upon exposure of leukocytes to a number of extracellular stress stimuli.[1–4] Although a number of structurally different inhibitors have been reported[5] to inhibit p38 with varying degrees of selectivity, none has reached commercial status.[6] This communication describes the utilization of 2-aryl pyridazinone as a suitable template for design of novel, selective p38 inhibitors.

VX-745 (**1**)[7] and its congeners[8] (Fig. 1) are potent and highly selective inhibitors of p38 MAP kinase. They have been shown to occupy the ATP binding site of p38 MAP kinase in a unique fashion.[9] The carbonyl group of these inhibitors induces a re-orientation of the amide bond between Met-109 and Gly-110 in the hinge region in order to form a dual hydrogen bond interaction. In almost all closely related kinases the residue adjacent to Met-109 bears a larger side chain which prevents facile amide bond re-orientation. A second hydrogen bond, thus, cannot be formed leading to poor binding affinity of these compounds for other kinases. The origin of the reported more than 1000-fold selectivity exhibited by these inhibitors is attributed to this sui generis 'peptide flip' in combination with a small Thr-106 'gate-keeper' residue lining the characteristic hydrophobic pocket attainable only by α and β isoforms of p38 MAP kinase.

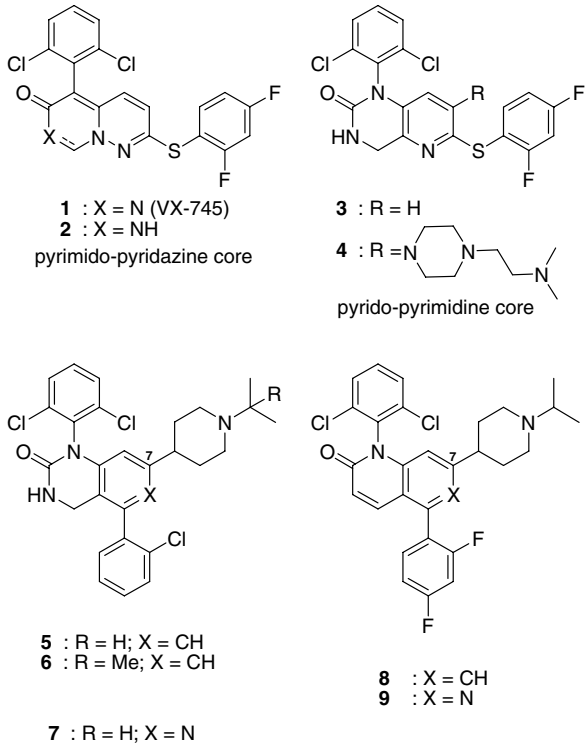

Figure 1. Novel p38 inhibitors: **VX-745** and homologs.

Keywords: p38 Inhibitors; MAP Kinase.
* Corresponding author. Tel.: +1 732 594 0939; e-mail: ravi_natarajan@merck.com

0960-894X/$ - see front matter © 2006 Elsevier Ltd. All rights reserved.
doi:10.1016/j.bmcl.2006.08.074

Inhibitor design began with an analysis of X-ray crystallographic data and site-directed mutagenesis studies.[10] Thus, two essential structural elements are required of a putative p38 inhibitor. First, a carbonyl group should be utilized as the anchor point. The kinase restructuring induced upon binding with the carbonyl group is critical for selectivity. Second, an aryl substituent suitably tethered to the main scaffold that enables its entry into the characteristic hydrophobic pocket-1, the entrance to which is lined by gate-keeper residue Thr-106. In addition to the above, occupation of a second partial hydrophobic pocket is expected to enhance potency and provide a handle for the manipulation of physical properties.

Selection criteria for an appropriate scaffold were driven by the net dipole moment contributed by the designed template. The hinge region peptide backbone in p38 MAP kinase is organized in a staggered arrangement of the amide bonds as expected in the natural state. A re-orientation of the amide bond between Met-109 and Gly-110 is required in order to accommodate the carbonyl anchor of any designed inhibitor (Fig. 2). It is proposed that the re-organization of amide dipoles within the peptide backbone becomes facile with templates characterized by a high dipole moment. Credence for this proposal can be gleaned from a simple comparison of p38 inhibitory activities of structurally isomeric compounds **2** and **3** (Fig. 1). Both are expected to make similar contacts in the p38 active site thereby implying equipotency. However, **2** inhibits p38 (IC_{50} of 0.8 nM) with 30-fold greater binding affinity than **3** (IC_{50} of 30 nM). The net dipole moments for the scaffolds pyrimido-pyridazinone and pyrido-pyrimidone in **2** and **3**, respectively, are calculated to be 9.2 and 3.0 Debye units, respectively.[11] It can be speculated that the substantially higher dipole in **2** enables a much more facile re-orientation of amide dipoles in the hinge region and contributes to the stability of the re-organized peptide backbone resulting in higher binding affinity. The considerations outlined above, in part, led to design of 2-pyridazinone based inhibitors.[11] It is expected that 2-pyridinones and 4-pyridinones can also be used similarly.[11]

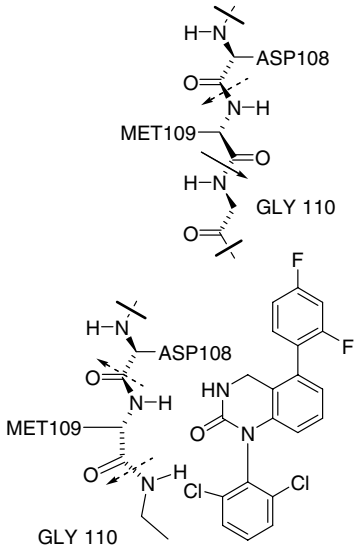

Figure 2. Representation of inhibitor induced re-orientation of hinge region of p38-MAP kinase.

The choice of a 2-chlorophenyl or 2,6-dichlorophenyl group as the substituent that is expected to occupy hydrophobic pocket 2 was based on prior SAR history.[8] The synthesis of pyridazine-based scaffold is shown in Scheme 1. Thus, condensation of maleic anhydride with 2-chlorophenyl hydrazine gave hydroxy pyridazinone derivative **10** which was treated with phosphorus oxychloride at reflux to furnish the chloro derivative **11**. Displacement of the chloride was expected to provide an avenue to explore the requirement of a suitable tether carrying the hydrophobic substituent. Other analogs were synthesized in a similar fashion. Several approaches to gain access of the hydrophobic pocket-1 were explored. Biaryls such as **14a** and **14b** did not inhibit the kinases (no activity at 20 μM). One-atom tethers such as aryl amines, aryl sulfides and aryl ethers gave promising results (Table 1). Aryl amines **15**, **17**, and **18** register IC_{50}s in the half-micromolar range. Small alkyl groups, chlorine, and fluorines were tolerated, while larger substituents such as methoxy and phenyl groups

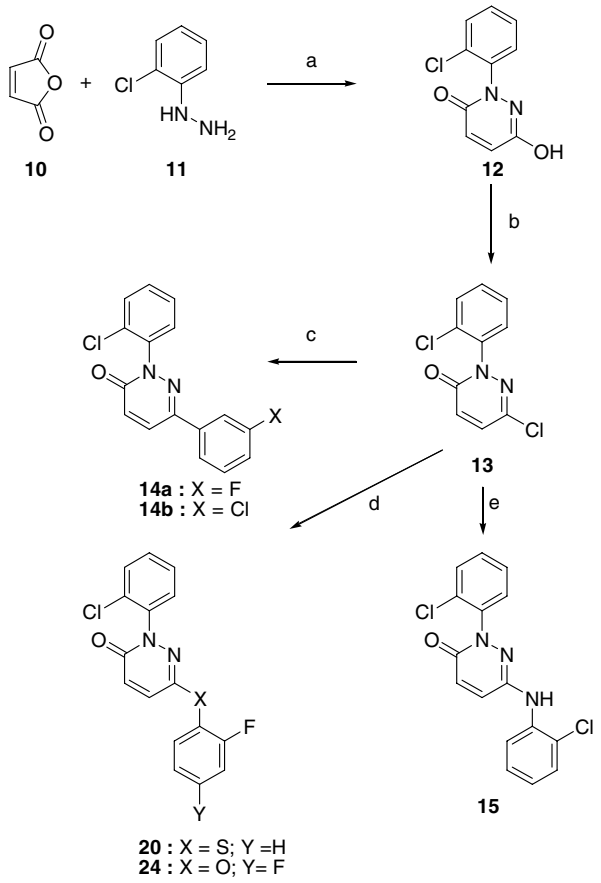

Scheme 1. General synthesis of pyridazinone scaffolds. Reagents and conditions: (a) EtOH, reflux 12 h, 70%; (b) $POCl_3$, 120 °C, 10 h, 82%; (c) 1.2 equiv of boronic acid, 2.5 equiv of Cs_2CO_3, 0.1 equiv of $Pd(0)(PPh_3)_4$, DMF/H_2O (4:1, v/v), 100 °C, 2 h, 80%; (d) 2.5 equiv of 2-F–Ph–SH or 2,4-di-F–PhOH, 2.5 equiv of Cs_2CO_3, DMF, 150 °C, 0.5 h, 65–79%; (e) 1.5 equiv of 2-Cl–Ph–NH_2, 0.1 equiv of $Pd_2(dba)_3$, 0.2 equiv of BINAP, 1.1 equiv of NaO-*t*-Bu, dioxane, 90 °C, 10 h, 65%.

Table 1. Accessing the hydrophobic pocket-1: explorations into optimal tether lengths and substituent requirements

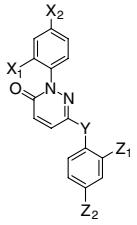

Compound	X_1	X_2	Y	Z_1	Z_2	p38-α (nM)	p38-β (nM)
15	Cl	H	NH	Cl	H	790	990
16	Cl	H	NH	Ph	H	NA	NA
17	Cl	H	NH	Et	H	560	NA
18	Cl	H	NH	Me	H	760	450
19	Cl	H	NH	OMe	H	2400	920
20	Cl	H	S	F	H	140	450
21	Me	Cl	S	F	F	310	850
22	Me	Cl	S	H	Cl	2000	NA
23	Cl	H	O	Cl	F	NA	NA
24	Cl	H	O	F	F	NA	NA
25	Cl	H	$NH–CH_2$	Me	H	3500	NA
26	Me	Cl	$O–CH_2$	CF_3	H	NA	NA

NA, no inh. at 20 μM. All numbers reported are mean of two independent titrations.

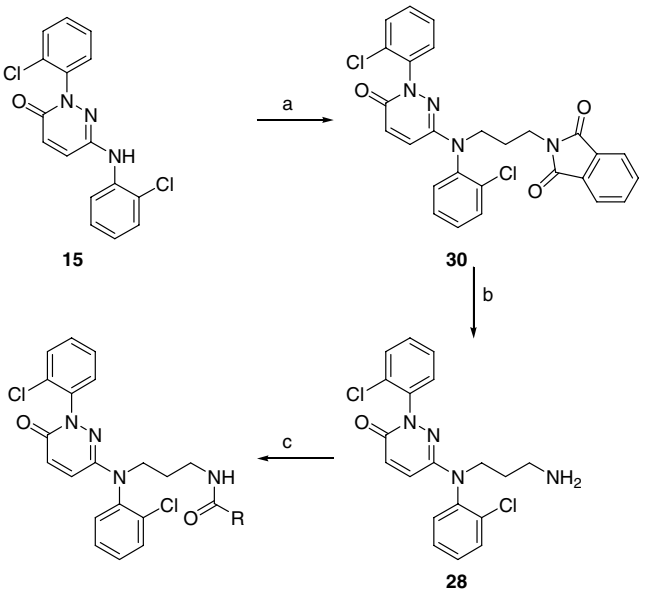

Scheme 2. Elaboration of aryl amine **15**. Reagents and conditions: (a) 1.5 equiv of NaH, 1.2 equiv of 3-Cl–propyl phthalimide, 0 °C, 3 h, 65%; (b) 5 equiv of NH_2NH_2, 75 °C, 2 h, 70%; (c) 1.2 equiv of R–COOH, 1.2 equiv of HOBt, 2.0 equiv of EDC, 2.0 equiv of TEA, rt, 10 h.

were clearly detrimental. Aryl sulfide **20** inhibited both isoforms of p38 (α and β) with an IC_{50} 140 and 450 nM, respectively. Aryl sulfides with a chlorine substitution in the para position (**22**) is sixfold less potent than corresponding fluorine analog. It was surprising that none of the aryl ethers (**23** and **24**) displayed any p38 inhibitory activity even though comparable aryl amines were potent. It is thought that the inherent lack of rotational bias and physical inability to access the hydrophobic pocket might contribute to its lack of activity. Two-atom tethers (**25** and **26**) were sub-optimal. Based on modeling aryl amine **15** and aryl sulfide **20** within the active site of p38, it was observed that the glycine-rich loop does not interact with the inhibitor. It was also conceived that elaboration under this loop will pre-orient the aryl substituent for facile entry into the hydrophobic pocket-1. Making contact with Asp-168 situated 6–9 Å from the one-atom tether affords another opportunity to enhance potency by means of a salt bridge (Scheme 2).

Aryl amine **15** provided a convenient starting point for exploring these ideas. The phthalimide derivative **30** with a 3-carbon linker was found to be surprisingly potent against both p38-α and p38-β. Corresponding 2C linker was not optimal. Unravelling the phthalimide yielded **28** with a concomitant drop-off in potency. The phthalimide moeity is thought to be involved in a π–π stacking interaction with tyrosine residue-35 on the G-rich loop. Figure 3 represents an X-ray crystal structure section of the complex between unactivated p38 and **30**.[12] The G-rich loop is highlighted in green color. The face-to-face interaction made by the pendant Tyr-35 in the G-rich loop with the phthalimide moiety

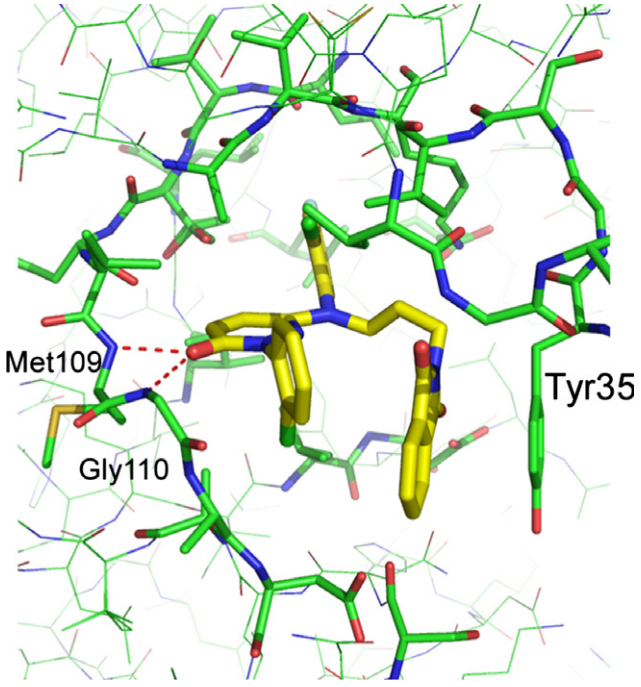

Figure 3. X-ray Crystal structure of p38-α in complex with **30**.

of **30** is obvious. The lack of potency for the corresponding 2C linker can be explained due to its inability to access a favorable stacking interaction that the 3C analog **30** is able to achieve. It can also be speculated that mere occupation of the space under the G-rich loop is sufficient to pre-orient the 2-chlorophenyl substituent for facile access into the hydrophobic pocket thus leading to higher potencies.

Table 2. Potency augmentation on designed pyridazinone templated p38 inhibitors: SAR explorations to optimize interactions under the G-rich loop

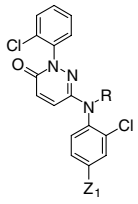

Compound	R	p38-α (nM)	p38-β (nM)
27[a]		168	135
28	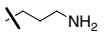	197	211
29	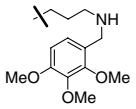	490	600
30	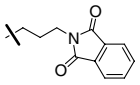	5	15
31[a]	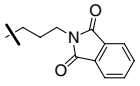	9	20
32	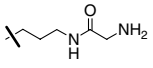	20	41
33	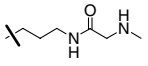	35	29
34	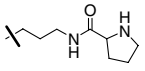	11	31
35	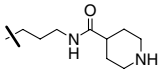	8	29
36	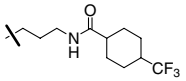	20	2

[a] Z_1 = H for all compounds except for **27** and **31** where Z_1 = F.

Due to the comparable potency of **28** with a 2C hydroxy analog **27**, it was assumed that the amine is not positioned to make a salt bridge with the proximal aspartic acid residue-168. In order to explore the facility of establishing this salt bridge amide analogs **32**–**35** were synthesized. Most of these compounds inhibited both isoforms of p38 with potency in the low nanomolar range. It is believed that the high potency displayed by these compounds primarily arises from their ability to occupy the space under the G-rich loop rather than through a salt bridge as the original intent for which they were designed for. The equipotency of designed analog **36**, which cannot form a salt bridge with proximal Asp-168, lends credence to the suggestion made above. It was also encouraging to note that analogs in Table 2 did not show any significant activity (no inh. at 10 μM) when screened against an extensive panel of known kinases particularly p38-γ, p38-δ, JNKs, and ERKs.

Thus, analysis of the binding modes of various p38 inhibitors has enabled the design of novel, potent, and selective p38 inhibitors based on a 2-aryl pyridazinone scaffold. Investigations to optimize pharmacokinetic profiles and functional activities are currently ongoing and are expected to yield compounds of clinical importance.

References and notes

1. Lee, J. C.; Laydon, J. T.; McDonnell, P. C.; Gallagher, T. F.; Kumar, S.; Green, D.; McNulty, D.; Blumenthal, M. J.; Heys, J. R.; Landvatter, S. W.; Stricker, J. E.; McLaughlin, M. M.; Siemens, J. R.; Fisher, S. M.; Livi, G. P.; White, J. R.; Adams, J. L.; Young, P. R. *Nature* **1994**, *372*, 739.
2. Han, J.; Lee, J.-D.; Bibbs, L.; Ulevitch, R. J. *Science* **1994**, *265*, 808.
3. Badger, A. M.; Bradbeer, J.; Votta, B.; Lee, J. C.; Adams, J. L.; Griswald, D. E. *J. Pharmacol. Exp. Ther.* **1996**, *279*, 1453.
4. For recent reviews, see (a) Rincon, M. *Curr. Opin. Immunol.* **2001**, *13*, 339; (b) Kumar, S.; Blake, S. M.; Emery, J. G. *Curr. Opin. Pharmacol.* **2001**, *1*, 307; (c) Muller-Ladner, U. *Curr. Opin. Rheumatol.* **1996**, *8*, 210; (d) Boehm, J. C.; Adams, J. L. *Exp. Opin. Ther. Pat.* **2000**, *10*, 25; (e) Henry, J. R.; Cavender, D. E.; Wadsworth, S. A. *Drugs Future* **1999**, *24*, 1345.
5. (a) Dominguez, C.; Powers, D. A.; Tamayo, N. *Curr. Opin. Drug Disc.* **2005**, *8*, 421; (b) Goldstein, D. M.; Gabriel, T. *Curr. Top. Med. Chem.* **2005**, *10*, 1017.
6. (a) Hynes, J.; Leftheris, K. *Curr. Top. Med. Chem.* **2005**, *10*, 967; (b) Salituro, F. G.; Germann, R. A.; Wilson, K. P.; Bemis, G. W.; Fox, T.; Su, MS-S. *Curr. Med. Chem.* **1999**, *6*, 807.
7. Bemis, G. W.; Salituro, F. G.; Duffy, J. P.; Harrington, E. M. US Patent 2000, 6,147,080.
8. (a) Natarajan, S. R.; Wisnoski, D. D.; Singh, S. B.; Stelmach, J. E.; O'Neill, E. A.; Schwartz, C. D.; Thompson, C. M.; Fitzgerald, C. E.; O'keefe, S. J.; Kumar, S.; Hop, C. E. C. A.; Zaller, D. M.; Schmatz, D. M.; Doherty, J. B. *Bioorg. Med. Chem. Lett.* **2003**, *13*, 273, and references within; (b) Stelmach, J. E.; Liu, L.; Patel, S. B.; Pivnichny, J. V.; Scapin, G.; Singh, S. B.; Hop, C. E. C. A.; Wang, Z.; Strauss, J. R.; Cameron, P. M.; Nichols, E. A.; O'keefe, S. J.; O'neill, E. A.; Schmatz, D. M.; Schwartz, C. D.; Thompson, C. M.; Zaller, D. M.; Doherty, J. B. *Bioorg. Med. Chem. Lett.* **2003**, *13*, 277; (c) Natarajan, S. R.; Wisnoski, D. D.; Thompson, J. E.; O'Neill, E. A.; O'Keefe, S. J.; Zaller, D. M.; Doherty, J. B. *Bioorg. Med. Chem. Lett.* **2006**, *16*, 4400; (d) Hunt, J. A.; Kallashi, F.; Ruzek, R. D.; Sinclair, P. J.; Ita, I.; McCormick, S. X.; Pivnichny, J. V.; Hop, C. E. C. A.; Kumar, S.; Wang, Z.; O'Keefe, S. J.; O'Neill, E. A.; Porter, G.; Thompson, J. E.; Woods, A.; Zaller, D. M.; Doherty, J. B. *Bioorg. Med. Chem. Lett.* **2003**, *13*, 467; (e) Natarajan, S. R.; Doherty, J. B. *Curr. Top. Med. Chem.* **2005**, *10*, 987.
9. (a) Wilson, K. P.; McCaffrey, P. G.; Hsiao, K.; Pazhanisamy, P.; Galullo, V.; Bemis, G. W.; Fitzgibbon, M. J.; Caron, P. R.; Murcko, M. A.; Su, M. S. S. *Chem. Biol.* **1997**, *4*, 423; (b) Wang, Z.; Canagarajah, B. J.; Boehm, J. C.; Kassisa, S.; Cobb, M. H.; Young, P. R.; Abdel-Meguid, S.; Adams, J. L.; Goldsmith, E. J. *Structure* **1998**, *6*, 1117; (c) Fitzgerald, C. E.; Patel, S. B.; Becker, J. W.;

Cameron, P. M.; Zaller, D.; Pikounis, V. B.; O'Keefe, S. J.; Scapin, G. *Nat. Struct. Biol.* **2003**, *10*, 764.
10. Wrobelski, S. T.; Doweyko, A. M. *Curr. Top. Med. Chem.* **2005**, *10*, 1017.
11. Partial charges and dipole moments were derived from the geometry optimization of each scaffold with the Hartree-Fock method using 6-31G** basis set. For further information see this URL: http://www.gaussian.com/citation_g03.htm. The calculated dipole moments of a pyridazinone, 2-pyridinone, and 4-pyridinone was 3.9, 4.7, and 7.1 Debye units, respectively.
12. Coordinates for the X-ray crystal structure have been deposited. Accession codes are rscb038982 and PDB ID is 2I0H.